Adsorption of O_2 on Ag(111): Evidence of Local Oxide Formation

B. V. Andryushechkin,[1,*] V. M. Shevlyuga,[1] T. V. Pavlova,[1] G. M. Zhidomirov,[1,2] and K. N. Eltsov[1]
[1]*A.M.Prokhorov General Physics Institute, Russian Academy of Sciences, ulitsa Vavilova 38, 119991 Moscow, Russia*
[2]*G.K.Boreskov Institute of Catalysis, Siberian Branch of the Russian Academy of Sciences, Prospect Lavrentieva 5,630090 Novosibirsk, Russia*
(Received 11 April 2016; revised manuscript received 7 June 2016; published 29 July 2016)

The atomic structure of the disordered phase formed by oxygen on Ag(111) at low coverage is determined by a combination of low-temperature scanning tunneling microscopy and density functional theory. We demonstrate that the previous assignment of the dark objects in STM to chemisorbed oxygen atoms is incorrect and incompatible with trefoil-like structures observed in atomic-resolution images in current work. In our model, each object is an *oxidelike* ring formed by six oxygen atoms around the vacancy in Ag(111).

DOI: 10.1103/PhysRevLett.117.056101

The interaction of molecular oxygen with the Ag(111) surface is one of the intriguing puzzles in surface science. The fundamental interest in the study of the O/Ag(111) system originates from the importance of silver catalysts for the selective oxidation of ethylene into ethylene oxide [1]. In their pioneering work, Rovida *et al.* [2] reported the formation of the Ag(111)-$p(4\times4)$-O superstructure at temperatures close to those used in real industrial processes. Since that time, research has largely been focused on the "solving" of the (4×4) structure [3–9].

In the 2000s, significant progress in the recognition of the O/Ag(111) system was achieved due to the application of scanning tunneling microscopy in combination with density functional theory (DFT) calculations [4–9]. As a result, the (4×4) structure has been solved [4–7,9]. Moreover, at low oxygen coverage, a new disordered phase of dark spots has been discovered on the Ag(111) surface [4,7,9]. Using DFT calculations, each dark spot has been assigned to the individual oxygen atom adsorbed in the fcc hollow site on the Ag(111) surface rather than to subsurface oxygen [8].

Though the model for the disordered phase has been widely accepted, there are important doubts in its validity. According to existing STM data, the oxygen coverage corresponding to the disordered phase is equal to 0.05–0.07 ML, which corresponds to the closest distance between two oxygen atoms of ≈10 Å [7]. However, it is not clear why further compression of the chemisorbed oxygen layer does not occur if the subsurface adsorption is excluded. In principle, a specific long-range repulsive interaction between oxygen atoms could be responsible for the prevention of formation of denser structures. However, the existence of such an interaction is unlikely.

In this Letter, we present new high-resolution STM images of the disordered oxygen phase on Ag(111) demonstrating trefoil structures (Fig. 1) instead of simple dark spots [7,9]. Using DFT calculations, we have shown that each object previously assigned to a chemisorbed oxygen atom is an oxidelike ring formed by six oxygen atoms around the vacancy in Ag(111). The resulting coverage for the disordered phase was found to be six times larger than in the previous model [7].

All experiments were carried out in an UHV setup containing LT-STM GPI CRYO [10] operating at 5–77 K, a cylindrical mirror analyzer, and LEED optics. A high-pressure reactor attached to the main setup allowed introduction of molecular oxygen up to 10 Torr keeping the sample temperature in the range of 300–600 K. The silver (111) sample was prepared by repetitive circles of Ar^+ bombardment (600 eV) and annealing up to 800 K. Oxygen introduction on Ag(111) was done at temperatures

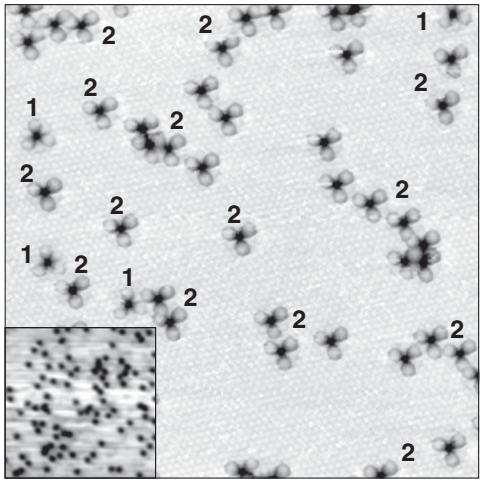

FIG. 1. STM image (187×187 Å^2, $U_s = 1737$ mV, $I_t = 0.5$ nA, 77 K) obtained after molecular oxygen exposure (1×10^{-1} Torr $\times$ 30 s, 433 K) on Ag(111) demonstrating the trefoil-like objects on the background of the Ag(111) lattice ("atomic-resolution" state of the tip). The concentration of the objects corresponds to the coverage of 0.028 ML. The inset shows the STM frame of the same size as the main image but showing the objects as dark spots ("normal" state of the tip).

of 300 K and 433 K by the backfilling of the chamber by O_2 with pressure in the range of $10^{-4} - 1$ Torr.

All DFT calculations have been performed by using the VASP package [11,12] with the Perdew-Burke-Ernzerhof (PBE) exchange-correlation functional [13] and van der Waals correction developed by Grimme (DFT-D2) [14]. The silver (111) substrate was modeled by a four layer slab with a (7×7) surface unit cell. During structure optimizations two upper layers of Ag atoms as well as the oxygen atoms were allowed to relax, while the bottom two layers of Ag were held fixed. We used a Monkhorst-Pack k-point grid of $5 \times 5 \times 1$ and 14 Å vacuum region between the slabs. STM simulations were performed within the Tersoff-Hamann approximation [15].

We have found that experimental STM images acquired at the initial stage of the Ag(111) oxidation at 433 K contain an array of similar objects forming a disordered phase. As a rule, these objects were imaged in STM as dark depressions with a diameter of 8–10 Å, in agreement with previous STM observations in Refs. [7,9] ("normal" state of the STM tip). Note also that similar pictures could be obtained after adsorption of O_2 at 300 K. Moreover, we also carried out STM measurements at room temperature and found that the dark features did not move. This observation is not in line with assigning these features to chemisorbed oxygen atoms, since surface diffusion of single oxygen atoms at 300 K should be noticeable [16].

At a certain state of the STM tip, we have been able to obtain atomic-resolution STM images which reveal the trefoil-like objects instead of the depressions (see Fig. 1). For comparison, the STM image of the same surface obtained with a tip in the "normal" state is shown in the inset to Fig. 1. It is noteworthy that influence of the tip shape may be ruled out since two types of differently oriented trefoils (marked as 1 and 2 in Fig. 1) exist on the surface. Usually, each tip starts working in the normal mode and switches to the "atomic-resolution" state as a result of the scanning close to the surface (low bias voltage). Therefore, the normal state of the tip likely corresponds to a clean tip, while the atomic-resolution state is related to a tip with an adsorbate (e.g., oxygen atom).

An important finding concerns the position of the center of the trefoil. According to the STM image in Fig. 2, it perfectly corresponds to the position of the atom in the upper Ag(111) layer. Therefore, an oxygen atom should occupy on-top, subsurface (tetra), or substitutional (in vacancy) positions.

According to DFT calculations, the on-top configuration does not correspond to the local minimum. After optimization of the coordinates, the oxygen atom moves to the most favorable fcc position (adsorption energy of −0.67 eV per atom). The subsurface (tetra) and substitutional (in vacancy) configurations were found to be less favorable than the fcc one. Simulated STM images for both models are not in line with the experiment, since they demonstrate a bright protrusion and a single depression, respectively. In addition, the existence of two types of trefoils with different orientation cannot be explained within a single oxygen atom model.

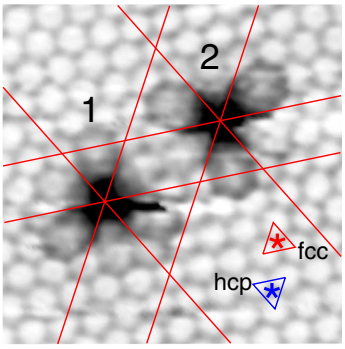

FIG. 2. Atomic-resolution STM image (30×30 Å^2) showing two types of trefoil structures with a high magnification. Red lines indicate close-packed atomic rows of Ag(111). Fcc and hcp adsorption sites are indicated by red and blue stars, respectively.

In further calculations, we have tested a series of structural models containing several oxygen atoms (see Fig. 3). First, we put three oxygen atoms around the vacancy in the upper Ag(111) layer [Fig. 3(a)]. Although the simulated STM image reproduces the trefoil geometry, the trefoil seen in the simulated STM image is smaller in size than that observed in the experiment. The same result was obtained for the reverse configuration with three oxygen atoms in tetra positions around the vacancy in the Ag(111) lattice.

For further analysis, we have assumed that two structural elements of silver oxide like the Ag_3O_4 pyramid and the oxide ring can be formed on the surface. We considered the subsurface [Fig. 3(b)] and on-surface [Fig. 3(c)] pyramid configurations. However, no correspondence with the experimental STM images was found for these cases.

Figures 3(d) and 3(e) show models in which six oxygen atoms are arranged in oxide-ring structures around the vacancy in the upper Ag(111) layer. In Fig. 3(d), the oxide ring is formed by three oxygen atoms in hcp positions and three oxygen atoms in subsurface octa positions. In the reverse configuration shown in Fig. 3(e), three oxygen atoms occupy fcc positions and another three oxygen atoms appear to be in subsurface tetra positions. STM images simulated for configurations in Figs. 3(d) and 3(e) correspond quite well to the experimental trefoils. Note that both hcp-octa and fcc-tetra configurations have similar adsorption energies (−0.76 eV and −0.75 eV, respectively) and appear to be the most energetically favorable of all the configurations considered in Fig. 3 and the on-surface fcc configuration.

Adding the oxygen atom in the center of the oxide ring [Figs. 3(f) and 3(g)] leads to the appearance of a white protrusion in the core of the trefoil in the simulated STM image, which is obviously not in line with the experiment. In the final model, we put nine oxygen atoms around the

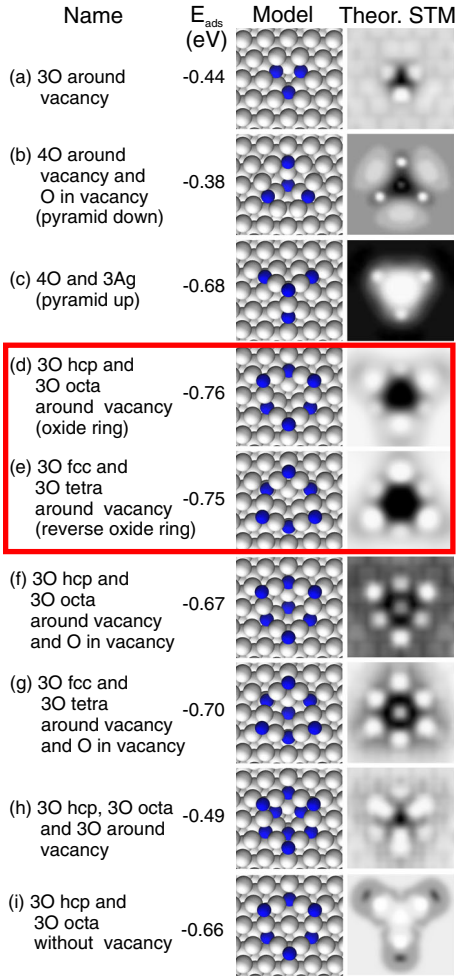

FIG. 3. (a)–(i) DFT modeling of the trefoil structures. The optimized geometry and the theoretical STM image (bias voltage of +1.7 V) are shown for each structural model. The adsorption energy is also indicated. Two favorable configurations, (d) and (e), are marked by the red rectangle.

vacancy in the Ag(111) layer. Although the simulated STM image contains a trefoil-like feature, the structure appears less energetically favorable than the models in Figs. 3(d) and 3(e). Thus, our DFT calculations point to the models containing an oxidelike ring around a silver vacancy. In addition, we have considered other models containing several oxygen atoms without a vacancy in the Ag(111) lattice [see, for instance, Fig. 3(i)]. However, no depression in the middle of the trefoil is reproduced in simulated STM images in all these cases.

To assign the fcc-tetra and hcp-octa models to the experimentally observed trefoils is not a simple task, since it requires knowledge of the orientation of the silver crystal. However, this problem can be solved by the adsorption of molecular chlorine on Ag(111). Indeed, the orientation of the crowdions in the $(\sqrt{3} \times \sqrt{3})R30°$ lattice of chlorine (three star interstitial objects [17]) unambiguously determines the positions of fcc and hcp sites in the Ag(111) lattice. Using this approach, we were able to mark fcc and hcp positions in the atomic resolution STM image in Fig. 2(b). Since the lobes of the trefoil are related to oxygen atoms adsorbed in fcc or hcp positions, then we can conclude that trefoil 1 corresponds to the fcc-tetra configuration, while trefoil 2 to the hcp-octa configuration [see Fig. 3(f) and 3(g)]. The adsorption energy for the hcp-octa configuration appears to be somewhat higher than that for the fcc-tetra configuration (Fig. 3). This computational result is in line with the experimental STM image in Fig. 1 showing mainly the trefoils of type 2.

Further confirmation of our model comes from the comparison of experimental and calculated STM images for the different bias voltages. Figure 4 shows the experimental and theoretical STM images of the hcp-octa trefoil for U_s equaled to −1.5 V, +1.7 V, and +3.0 V. For the bias voltage of +1.7 V, there is a perfect correspondence between the model and the experiment. In experimental STM images at voltages exceeding +3 V, the oxide rings look like bright rings with a small depression in the middle. At − 1.5 V, the shape of the lobes of the trefoil changes [see Fig. 4(c)]. According to Fig. 4, all the principal features of the STM images can be reproduced quite well within our model.

Although three of six oxygen atoms in the trefoils occupy on-surface (fcc or hcp) positions, one should consider the oxide ring around the vacancy to be a special object (local silver oxide). Indeed, a trefoil always consists of three lobes and no defect trefoil structures have been observed in STM images. This observation means that only the configuration of six oxygen atoms is stable. We calculated the adsorption energy for a system containing a vacancy and six oxygen atoms randomly adsorbed in fcc positions within the same unit cell as in calculations from Fig. 3. Such a configuration ($E_{ads} = -0.68$ eV) appears to be less favorable than the trefoil structures shown in Figs. 3(d) and 3(e). Therefore, we conclude that the existence of separate chemisorbed oxygen atoms on Ag(111) is unfavorable.

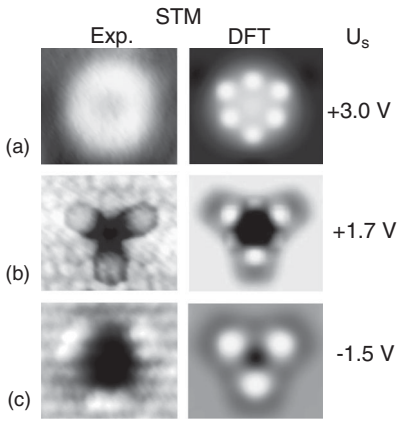

FIG. 4. The bias dependence of the experimental and theoretical STM images for the trefoil structure (model hcp-octa). (a) $U_s = +3$ V; (b) $U_s = +1.7$ V; (c) $U_s = -1.5$ V.

For further characterization of obtained structures, we performed DFT calculations of vibrational modes for both fcc-tetra (1) and hcp-octa (2) configurations. We found out the presence of the vibrational modes which are comparable to those in silver oxides structures: Ag_2O and AgO. In particular, the fcc-tetra trefoil exhibits modes at 49–54 meV, 59–61 meV, and 66–67 meV, being comparable with vibrations characteristic of the Ag_2O structure: 53 meV [18], 61 meV, [18] and 66–67 meV [18–20]. The hcp-octa trefoil, in turn, exhibits modes at 55 meV and 58–61 meV, being in the range of modes characteristic of AgO (53 meV, 58 meV and 61 meV [18]). There is a correlation between our data and the oxygen configurations in oxides structures. In particular, in Ag_2O, the oxygen atom is in the tetrahedron interstitial position similar to that in the fcc-tetra trefoil. On the other hand, in the AgO crystal, the oxygen atom occupies the off-center octahedral site similar to some extent to the octa position in the hcp-octa trefoil.

Now we can make a bridge to existing HREELS data obtained for oxidized Ag(511) and Ag(210) surfaces containing different types of steps [21]. In Ref. [21], the authors reported the experimental detection of oxidelike modes in HREELS. In particular, for the Ag(511) surface the mode 68 meV was observed, while for the Ag(210) surface, the spectra contained a peak at 53 meV. The authors made a link between different oxygen configurations on Ag(511) and Ag(210) surfaces and two possible oxide structures (Ag_2O and AgO). Their general conclusion was that at initial stages of the oxidation process, the stoichiometry of surface oxide can be tuned by the geometry of the steps. Thus, the comparison of our data and HREELS data by Savio *et al.* [21] shows that formation of local oxide structures at the initial stage of silver oxidation is quite a general phenomenon. Of course, the type of local oxide depends on the structure and symmetry of the silver plane.

The formation of the vacancies in the Ag(111) lattice is an important step towards the formation of trefoil structures. We believe that this process is induced by the adsorption of oxygen atoms, since recent DFT calculations by Jones *et al.* [22] indicate a notable decrease of the surface vacancy formation energy (down to ≈0.1–0.2 eV) near the oxygen atom placed in either an on-surface or a subsurface position on Ag(111) [22].

It is noteworthy that disordered structures to some extent similar to those observed in the present study have been observed by STM on oxidized Ag(100) and Ag(110) surfaces [23–26]. Since no atomic resolution was achieved, we can not exclude the formation of more complex oxygen objects similar to oxide rings found in the present study.

In summary, we have presented a STM and DFT study of the disordered oxygen phase formed on the Ag(111) surface at low coverages. We demonstrate that dark depressions previously assigned to individual oxygen atoms may be described by oxidelike rings around vacancies in the upper Ag(111) layer. The preferable configuration (hcp-octa model) contains the vacancy in the Ag(111) lattice surrounded by three oxygen atoms in hcp positions and three oxygen atoms in subsurface octa positions. The oxygen coverage corresponding to the saturation of the disordered phase appears to be 6 times larger than in the older models.

This work was supported by Grant No. 16-12-10546 from the Russian Science Foundation. We are grateful to the Joint Supercomputer Center of RAS and to the Supercomputing Center of Lomonosov Moscow State University [27] for the possibility of using their computational resources for our calculations.

*andrush@kapella.gpi.ru

[1] J. G. Serafin, A. C. Liu, and S. R. Seyedmonir, J. Mol. Catal. A: Chem. **131**, 157 (1998).
[2] G. Rovida, F. Pratesi, M. Maglietta, and E. Ferroni, J. Vac. Sci. Technol. **9**, 796 (1972).
[3] A. Michaelides, K. Reuter, and M. Scheffler, J. Vac. Sci. Technol. A **23**, 1487 (2005) and references therein.
[4] C. I. Carlisle, D. A. King, M. L. Bocquet, J. Cerdá, and P. Sautet, Phys. Rev. Lett. **84**, 3899 (2000).
[5] J. Schnadt, A. Michaelides, J. Knudsen, R. T. Vang, K. Reuter, E. Lægsgaard, M. Scheffler, and F. Besenbacher, Phys. Rev. Lett. **96**, 146101 (2006).
[6] M. Schmid, A. Reicho, A. Stierle, I. Costina, J. Klikovits, P. Kostelnik, O. Doubay, G. Kresse, J. Gustafson, E. Lundgren, J. N. Anderson, H. Dosch, and P. Varga, Phys. Rev. Lett. **96**, 146102 (2006).
[7] C. Carlisle, T. Fujimoto, W. Sim, and D. King, Surf. Sci. **470**, 15 (2000).
[8] A. Michaelides, M.-L. Bocquet, P. Sautet, A. Alavi, and D. King, Chem. Phys. Lett. **367**, 344 (2003).
[9] J. Schnadt, J. Knudsen, X. L. Hu, A. Michaelides, R. T. Vang, K. Reuter, Z. Li, E. Lægsgaard, M. Scheffler, and F. Besenbacher, Phys. Rev. B **80**, 075424 (2009).
[10] http://www.sigmascan.ru.
[11] G. Kresse and J. Hafner, Phys. Rev. B **47**, 558 (1993).
[12] G. Kresse and J. Furthmüller, Phys. Rev. B **54**, 11169 (1996).
[13] J. P. Perdew, K. Burke, and M. Ernzerhof, Phys. Rev. Lett. **77**, 3865 (1996).
[14] S. Grimme, J. Comput. Chem. **27**, 1787 (2006).
[15] J. Tersoff and D. R. Hamann, Phys. Rev. B **31**, 805 (1985).
[16] Y. Kunisada, H. Nakanishi, W. A. Diño, and H. Kasai, J. Phys. Conf. Ser. **379**, 012013 (2012).
[17] B. V. Andryushechkin, V. V. Cherkez, B. Kierren, Y. Fagot-Revurat, D. Malterre, and K. N. Eltsov, Phys. Rev. B **84**, 205422 (2011).
[18] G. I. N. Waterhouse, G. A. Bowmaker, and J. B. Metson, Phys. Chem. Chem. Phys. **3**, 3838 (2001).
[19] B. Pettinger, X. Bao, I. Wilcock, M. Muhler, R. Schlögl, and G. Ertl, Angew. Chem., Int. Ed. Engl. **33**, 85 (1994).
[20] T. Lan, C. W. Li, J. L. Niedziela, H. Smith, D. L. Abernathy, G. R. Rossman, and B. Fultz, Phys. Rev. B **89**, 054306 (2014).

[21] L. Savio, C. Giallombardo, L. Vattuone, A. Kokalj, and M. Rocca, Phys. Rev. Lett. **101**, 266103 (2008).
[22] T. E. Jones, T. C. R. Rocha, A. Knop-Gericke, C. Stampfl, R. Schlögl, and S. Piccinin, Phys. Chem. Chem. Phys. **16**, 9002 (2014).
[23] T. Zambelli, J. V. Barth, and J. Wintterlin, J. Phys. Condens. Matter **14**, 4241 (2002).
[24] I. Costina, M. Schmid, H. Schiechl, M. Gajdos, A. Stierle, S. Kumaragurubaran, J. Hafner, H. Dosch, and P. Varga, Surf. Sci. **600**, 617 (2006).
[25] M.-F. Hsieh, D.-S. Lin, H. Gawronski, and K. Morgenstern, J. Chem. Phys. **131**, 174709 (2009).
[26] M. Smerieri, L. Savio, L. Vattuone, and M. Rocca, J. Phys. Condens. Matter **22**, 304015 (2010).
[27] V. Sadovnichy, A. Tikhonravov, Vl. Voevodin, and V. Opanasenko, in *Contemporary High Performance Computing: From Petascale toward Exascale*, edited by J. S. Vetter (CRC Press, Boca Raton, 2013), pp. 283–307.